

A dual catalyst bed for the autothermal partial oxidation of methane to synthesis gas

G. C. M. Tong, J. Flynn, and C. A. Leclerc*

Department of Chemical Engineering, McGill University, 3610 University St., Montréal, Québec, H3A 2B2 Canada

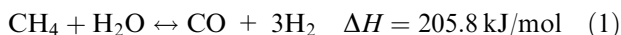
Received 21 January 2005; accepted 12 April 2005

Dual bed catalysts were found to produce high yields (>85%) of hydrogen from methane and air in a millisecond contact time reactor. The dual bed catalyst consisted of a 5 mm platinum combustion catalyst followed by a 5 mm nickel steam reforming catalyst. The platinum catalyst was used to totally oxidize approximately one-quarter of the methane feed to carbon dioxide and water. In the nickel catalyst, the carbon dioxide and water reformed the remaining methane to hydrogen and carbon monoxide. This process is favored at high flow rates, because the heat generated in the platinum catalyst is convected to the nickel catalyst at a higher rate. The heat delivered to the nickel catalyst favors the endothermic reforming reactions that generate the hydrogen and carbon monoxide.

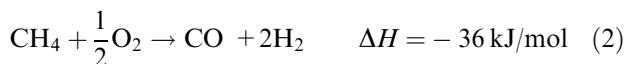
KEY WORDS: hydrogen; partial oxidation; catalysts; syngas; platinum; nickel; fuel processing; millisecond reactor.

1. Introduction

Catalytic partial oxidation (CPO) has shown much promise as an alternative process to steam reforming to generate hydrogen for fuel cells and syngas for methanol and Fischer–Tropsch synthetic fuels. However, steam reforming is used in industrial hydrogen production.



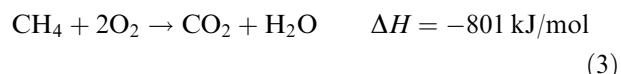
It is carried out in tubes packed with a nickel catalyst [1]. Since the reaction is endothermic, the tubes are placed in a furnace for heating up to ~800 °C. The process requires a residence time on the order of a second to achieve high yields of hydrogen. CPO, a fuel rich oxidation, has received much attention in the literature [2–5].



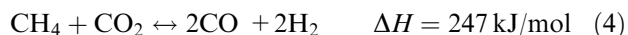
The process can be carried out over a fixed bed catalyst at residence times on the order of 1 ms [5, 6]. Since the reaction is exothermic, once the catalyst undergoes ignition, it remains lit off as long as reactants are fed. For fuel cell applications, this system is particularly attractive due to its rapid transient response at start-up [7, 8]. In addition, this system has proven to be robust by handling a wide array of fuels, including methane [9], ethanol [10], *i*-octane [11], and *n*-decane [12, 13], the last two being single component model compounds for gasoline and diesel respectively. It has been found that rhodium gives the highest yield of hydrogen for CPO

[14]. It is stable for many hours and achieves greater than 90% selectivity of hydrogen and greater than 90% conversion of methane. Unfortunately, rhodium is an expensive metal with a history of unstable pricing. This work focuses on two sequential catalyst beds using different, cheaper metals to catalyze the CPO system.

Recent research has shown that the CPO process occurs in two steps [15, 16]. The first step is a deep oxidation (3) of one-quarter of the methane to make carbon dioxide and water, while using all of the oxygen.



This reaction is exothermic, so it generates large amounts of heat. The second step includes reforming of the remaining methane by water (1) and carbon dioxide (4).



Since the reforming reactions are endothermic, they use the heat generated in the first stage to form carbon monoxide and hydrogen. Based on this two step mechanism, it is theorized that instead of choosing catalysts based on the overall reaction (2), reactor performance can be increased by choosing metals based on the two-step mechanism. By operating with a combustion catalyst immediately followed by a reforming catalyst, methane conversion, hydrogen selectivity, and hence hydrogen yield should increase compared to a single catalyst that is optimal for the global reaction.

In this work, we have performed CPO experiments on a sequential bed catalyst made up of a platinum coated monolith for combustion followed immediately by a nickel coated monolith for reforming to produce synthesis gas. Platinum has shown to be an effective

*To whom correspondence should be addressed.
E-mail: corey.leclerc@mcgill.ca

combustion catalyst [17] without deactivating under CPO feed conditions [18]. As previously stated, nickel is used industrially for the steam reforming process.

The major benefit of using these two metals is that they are less expensive than rhodium. Figure 1 shows the price of platinum and rhodium since the advent of the catalytic converter [19, 20]. Since 1983, rhodium has always been more expensive than platinum except for a brief 2 year period in the mid 1990's. Rhodium tends to be more expensive than platinum and has been more unstable reaching a price of over \$3700US per troy ounce in 1991. In contrast, platinum prices have peaked under \$600US per troy ounce in 2003. At 2003 prices, the dual bed system costs about 40% of the price of the rhodium catalyst assuming only half as much platinum is needed compared to rhodium.

A considerable amount of research has focused on bimetallic catalysts of platinum and nickel, where the platinum and nickel were used in the same catalyst bed for combined CPO and steam reforming [21, 22]. The bimetallic catalyst did not compare very well with rhodium, since it only reached a hydrogen yield of 55% though at much different operating conditions. Other work has looked at sequential bed catalysts [23]. The research was carried out at lower GHSV's ($\sim 10,000 \text{ h}^{-1}$), with a different combustion catalyst, and was not operated auto-thermally, which is a key operating condition in this work. Their work was carried out with no dilution or with dilution in excess of nitrogen in air, whereas this work was carried out in air, a more practical oxidant.

We have tested a dual bed system (Figure 2a) for the production of synthesis gas. We tested two different dual bed catalysts over a wide range of feed stoichiometries and inlet flow rates. The catalysts included a 5 mm

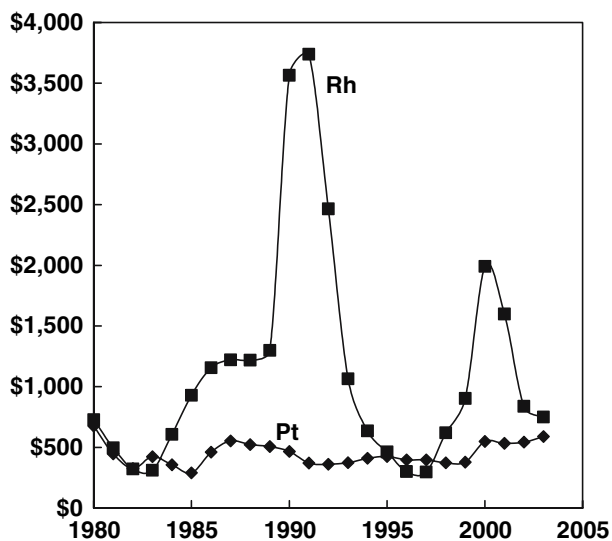


Figure 1. Average annual prices per troy ounce for rhodium and platinum from 1980 to the present as reported by the US Department of the Interior, US Geological Survey [19, 20].

platinum bed followed by a 5 mm nickel bed (Pt/Ni) catalyst and a 5 mm nickel bed followed by a 5 mm platinum bed (Ni/Pt) catalyst. The 5 mm Pt/Ni catalyst is our dual bed system described previously. The Ni/Pt catalyst, in which the feed gases contact the nickel bed prior to the platinum bed, was tested to prove the efficacy of having a combustion catalyst followed by a reforming catalyst in our dual bed system. Since nickel and platinum show some activity for combustion and reforming respectively, it is important to test the Ni/Pt performance. It is expected that this catalyst will perform poorly compared to the Pt/Ni catalyst, since nickel is not as good as platinum for combustion and platinum is not as good as nickel for reforming.

In addition, dual bed catalysts were compared to 10 mm single monolith platinum and rhodium catalysts (Figure 2b). All catalysts were tested over a wide range of feed ratios, reported as the methane to oxygen ratio, and flow rates. Increasing the flow rate has two effects on the system. It will lead to a shorter residence time, which may reduce methane conversion. However, this may be countered by increased heat transfer from the front of the catalyst to the back. This will aid our dual bed system, since heat generated in the combustion zone will be convected to the reforming zone faster at higher flow rates. The increased heat in the reforming zone will lead to a higher conversion of methane and a higher yield of hydrogen. If the flow rate is too high, it is

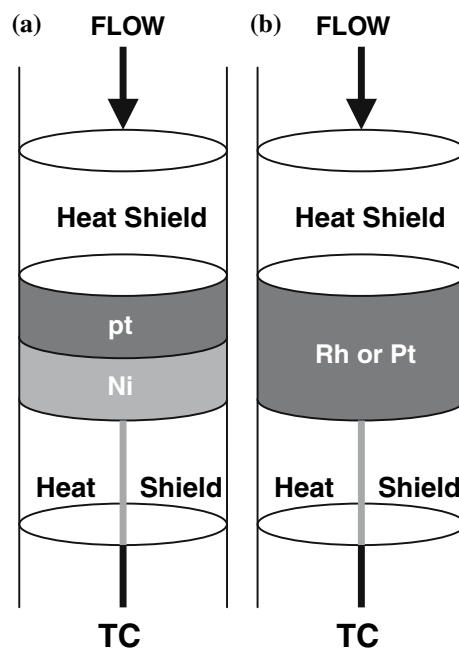


Figure 2. Schematics of the sequential bed catalysts (a) and the monometallic catalyst (b). The sequential bed catalysts are made up of two 5 mm monoliths. In this work, a platinum catalyst was followed by a nickel catalyst (shown) as well as a nickel catalyst followed by a platinum catalyst (not shown in Figure 2a). For the monometallic catalysts, 10 mm monoliths coated in rhodium or platinum were used.

possible that oxygen will not be completely converted, which will greatly reduce the heat generated in the system and negate the enhanced heat transfer.

2. Experimental

2.1. Apparatus

The experimental apparatus consisted of a quartz tubular reactor with an internal diameter of 18 mm. The catalyst was inserted between two blank monoliths with pore densities of 45 pores per inch (ppi) to limit heat loss from radiation in the axial direction. Monoliths were wrapped in Fiberfrax paper to prevent gas bypass. To avoid radial heat losses, the reactor was insulated with an Isofrax blanket. The back face temperature was monitored by a K-type thermocouple placed between the end of the catalyst bed and the downstream heat shield. Dry air and methane flow rates were controlled by FC-261V and FC-260V Tylan mass flow controllers respectively. Product gases were analyzed by an Agilent 6890 gas chromatograph (GC) using a thermal conductivity detector (TCD). A HP-PLOT molesieve 5A column was used to separate methane, oxygen, nitrogen, and carbon monoxide, while a HP-PLOT Q capillary column separated carbon dioxide from the other gases. Balances on carbon atoms closed to within $\pm 5\%$.

2.2. Catalyst preparation

The catalysts were supported on α -alumina cylindrical foam monoliths with pore densities of 80 ppi, diameter of 17 mm, porosity of 0.83, and length of 10 mm for monometallic catalysts and two adjacent 5 mm for sequential bed catalysts. Each monolith was washcoated with γ -alumina. The washcoat loading varied between 2.8 and 7.7 wt%. Metal precursors, such as nickel (II) nitrate, hydrogen hexachloroplatinate, and rhodium (II) nitrate were deposited on the monoliths by the incipient wetness technique. After drying overnight, rhodium and nickel catalysts were calcined in air for 6 h at 600 °C and platinum for 5 h at 600 °C. Metal loadings were 5.2 wt% for rhodium, 3.2 wt% for platinum, and 2.1/3.6 wt% for the bimetallic Pt/Ni and Ni/Pt catalysts.

2.3. Ignition and shutdown

Reaction start-up was initiated by heating the apparatus with a Bunsen burner. Catalyst ignition is associated with a jump in the back face temperature. The typical light-off temperature was less than 300 °C. Once the catalyst ignited, the Bunsen burner was removed and the reactor was insulated. To shut down the reactor, the flow rate of air was turned off first before methane in order to avoid the formation of an explosive mixture.

2.4. Reactor performance

Reactor performance is based on four different parameters: reactant conversion, product selectivity, product yield, and gas hourly space velocity.

2.4.1. Conversion, selectivity, and yield

The conversion of molecule i is defined as the ratio of the amount reacted by the amount fed:

$$X_i = \frac{F_{i,\text{in}} - F_{i,\text{out}}}{F_{i,\text{in}}}$$

where $F_{i,\text{in}}$ is the flow rate of species i in the feed and $F_{i,\text{out}}$ is the flow rate of species i in the outlet.

The selectivity ($S_{i,j}$) of species i with respect to atom j is the amount of that species in the product stream divided by the stoichiometric sum of all products (k) based on the j (carbon or hydrogen) atom:

$$S_{i,j} = \frac{v_{i,j}F_{i,\text{out}}}{\sum_k v_{k,j}F_{k,\text{out}}}$$

where $S_{i,j}$ is the selectivity of product i with respect to atom j , $v_{i,j}$ is the stoichiometric amount of j atoms in species i , and $F_{i,\text{out}}$ is the flow rate of product i . In this work, molecular hydrogen selectivity is based on hydrogen atoms and carbon monoxide selectivity is based on carbon atoms.

The yield of a molecule is defined as the product of the methane conversion and the molecule selectivity.

2.4.2. Gas hourly space velocity

The gas hourly space velocity (GHSV) is calculated from the volumetric flow rate at standard conditions ($T = 25$ °C and $P = 1$ atm) divided by the void volume of the catalyst:

$$\text{GHSV} = \frac{\dot{V}}{\varepsilon V_{\text{monolith}}}$$

where \dot{V} is the volumetric flow rate at STP, ε is the monolith void fraction, and V_{monolith} is the volume of the monolith.

3. Results

3.1. Feed stoichiometry

Figure 3 shows plots of (a) back face temperature, (b) methane conversion, (c) hydrogen selectivity, and (d) carbon monoxide selectivity for experiments carried out at 220,000 h⁻¹ with methane to oxygen ratios varying from 1.7 to 2.1.

The back face temperature (Figure 3a) decreases by 50 °C for all four catalysts as the methane to oxygen ratio is increased from 1.7 to 2.1. Rhodium exhibits the lowest temperatures followed by Pt/Ni and platinum. The Ni/Pt catalyst experiences temperatures 100 °C higher than the other three catalysts.

The conversion of methane (Figure 3b) also decreases as the methane to oxygen ratio increases. Platinum shows a decrease in conversion of 17% from 88% to 71% over the range of methane to oxygen. Rhodium also shows a large decrease around 12% from 91% to 79%, whereas the two sequential catalysts show decreases of only 6% from 94% to 88% and 5% from 86% to 81% for Ni/Pt and Pt/Ni respectively. Over the entire range, the Pt/Ni catalyst has the highest conversion. The other three show overlap at different points in the range.

The selectivity of hydrogen (Figure 3c) and carbon monoxide (Figure 3d) show little change over the feed ratios investigated. Any changes that they exhibit are less than 5%, which are on the order of the carbon error. The rhodium catalyst exhibits slightly higher hydrogen

selectivities than the platinum and Pt/Ni catalysts. The Ni/Pt catalyst does not attain 85% selectivity. For all catalysts, the carbon monoxide selectivity ranges between 86% and 91% at all feed ratios.

3.2. Flow rate

Figure 4 shows plots of (a) back face temperature, (b) methane conversion, (c) hydrogen selectivity, and (d) carbon monoxide selectivity for experiments carried out at a methane to oxygen ratio of 1.7 at GHSV's ranging from 108,000 h⁻¹ to 281,000 h⁻¹. In all cases, the oxygen conversion was above 97%.

The back face temperature (Figure 4a) increases as the GHSV is increased for all catalysts except rhodium.

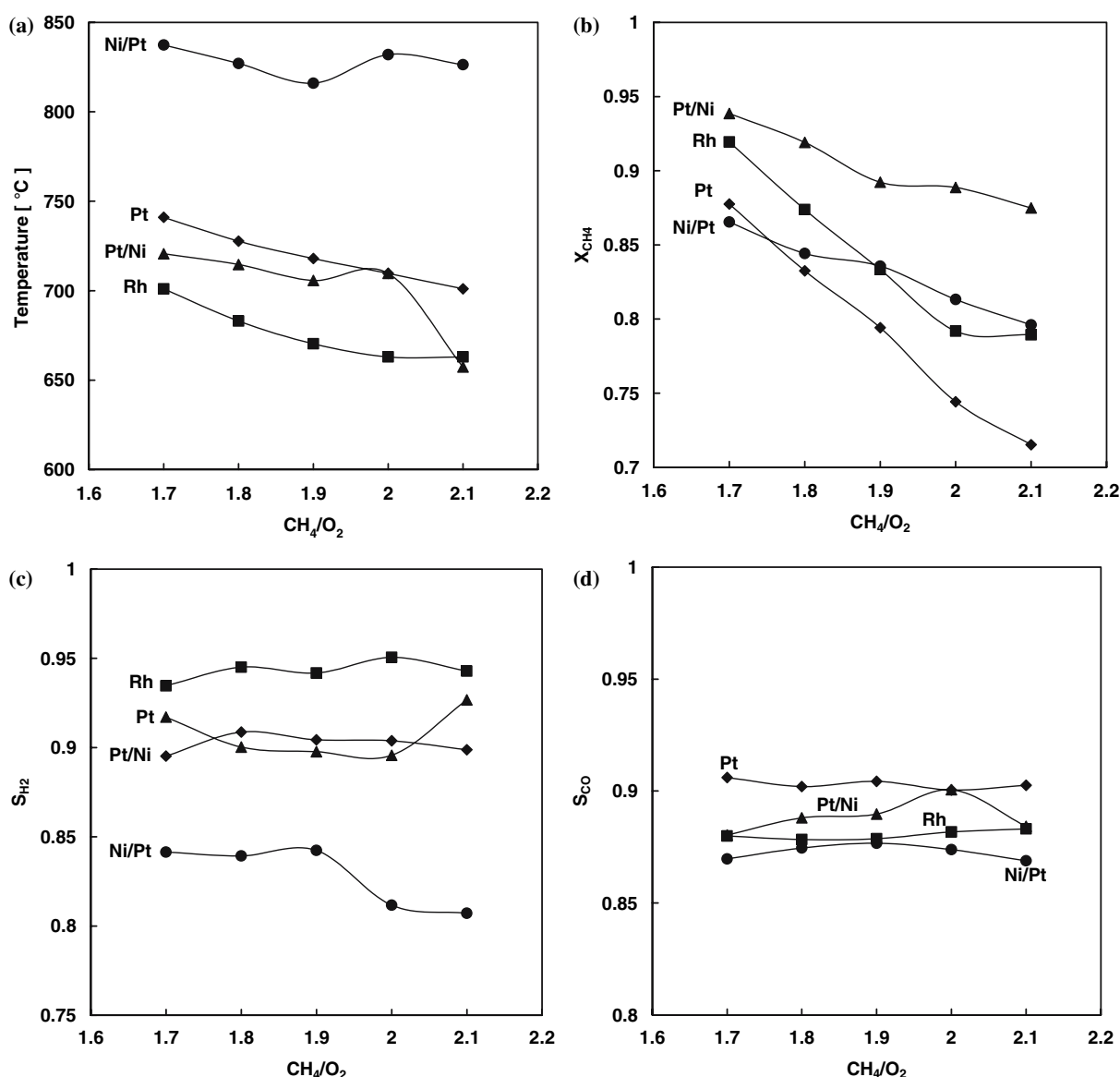


Figure 3. Back face temperature (a), methane conversion (b), hydrogen selectivity (c), and carbon monoxide selectivity (d) for the catalytic partial oxidation of methane performed in air over rhodium (■), platinum (◆), platinum/nickel (▲), and nickel/platinum (●) catalysts for varying methane to oxygen feed ratios at a GHSV of 220,000 h⁻¹. Lines are added to aid the visual presentation of the plot.

For rhodium, the temperature stays constant around 675–700 °C. The platinum and Pt/Ni catalysts exhibit temperature increases of approximately 50 °C and the Ni/Pt catalyst exhibits a temperature change of over 150 °C. The first three all exhibit back face temperatures from 675 to 775 °C, while the Ni/Pt catalyst exhibits much higher temperatures with an upper limit over 900 °C.

The methane conversion (Figure 4b) for all but rhodium showed obvious maxima. The Pt/Ni and Ni/Pt catalysts showed maxima around a GHSV of 220,000 h⁻¹ with Pt/Ni reaching a conversion of 94% and Ni/Pt reaching a conversion of 86%. Over the entire range the conversion varied from 87% to 94% at the peak to 91% for the Pt/Ni catalyst and from 81% to 86% at the peak to 75% for the Ni/Pt catalyst. The

platinum showed a maximum at 160,000 h⁻¹ ranging from 81% to 91% at the peak to 70% over the range of GHSV's investigated. The conversion of rhodium stayed nearly constant (91% to 93%) over the entire range that was investigated.

The hydrogen selectivities (Figure 4c) showed little change over the operating range for rhodium, platinum, and Pt/Ni. They experienced selectivities ranging from 90% to 95%, 91% to 88%, and 92% to 91% from low GHSV to high GHSV respectively. The Ni/Pt catalyst showed a constant decrease from 87% at the lowest GHSV to 77% at the highest GHSV.

The carbon monoxide selectivity (Figure 4d) for all four catalysts showed little change over the range of GHSV's. The platinum catalyst was the most selective for carbon monoxide over almost the entire range. The

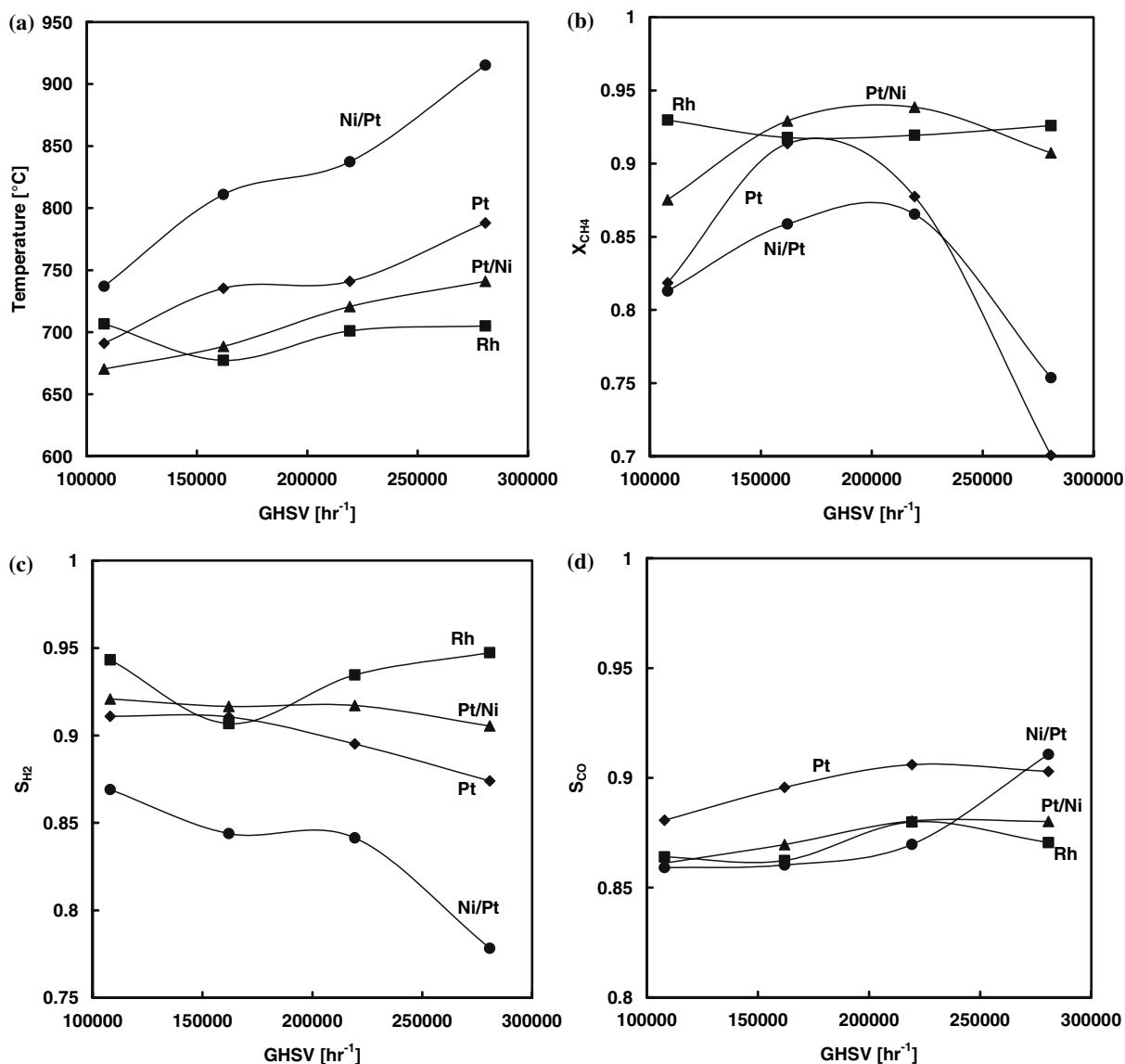


Figure 4. Back face temperature (a), methane conversion (b), hydrogen selectivity (c), and carbon monoxide selectivity (d) for the catalytic partial oxidation of methane performed in air over rhodium (■), platinum (◆), platinum/nickel (▲), and nickel/platinum (●) catalysts for varying gas hourly space velocities at a methane to oxygen feed ratio of 1.7. Lines are added to aid the visual presentation of the plot.

platinum, rhodium, and Pt/Ni catalysts all increased by about 1% over the range of GHSV's, while the Ni/Pt catalyst increased by about 5% from 86% to 91%.

3.3. Catalyst degradation

Since nickel is known to deactivate under CPO feed conditions, an experiment was run over 10 h at a methane to oxygen ratio of 1.7 and a GHSV of $220,000 \text{ h}^{-1}$. Since nickel loses activity in less than 10 h under CPO feed conditions [14], it was not necessary to run longer for this work. The reactant conversions, product selectivities, and back face temperature are shown in Figure 5. Over the entire time period the back face temperature changed by only 2°C staying at just under 700°C . The methane and oxygen conversions stayed nearly constant at $\sim 90\%$ for methane and $> 97\%$ for oxygen. The product selectivities showed little variation with hydrogen selectivity around 91% and carbon monoxide selectivity around 88%.

4. Discussion

The Pt/Ni catalyst performed nearly as well or as well as the rhodium catalyst over a wide range of operating conditions. The Pt/Ni catalyst achieved a hydrogen yield of 86% compared to the 88% hydrogen yield of the rhodium catalyst. The Pt/Ni catalyst in 2003 prices costs about 40% of the rhodium catalyst including blank monolith costs, while still giving similar hydrogen yields.

4.1. Pt/Ni versus Rh and Pt/Ni versus Pt

The goal of this research is to prove that it is possible to choose catalysts based on smaller reaction

subsets instead of just the overall reaction. In this work, a Pt/Ni catalyst was investigated for CPO (2) to target combustion reactions immediately followed by reforming reactions. The Pt/Ni catalyst achieved higher conversions, hydrogen selectivities, and hydrogen yields than the platinum catalyst as expected. The Pt/Ni catalyst compared favorably to the rhodium catalyst. For the experiments with varying feed ratios, the Pt/Ni catalyst exhibited 2–8% higher conversion of methane than the rhodium catalyst. The hydrogen selectivity for the Pt/Ni catalyst was from 1–4% smaller than the rhodium catalyst. The conversions and selectivities translate in nearly equal hydrogen yields for the two catalysts.

Perhaps the most interesting result is for the varying GHSV's. Both had similar trends in hydrogen selectivity with the rhodium slightly outperforming the Pt/Ni catalyst. However, for the methane conversion, Pt/Ni performs similarly to rhodium, but it encounters a maximum in methane conversion and rhodium does not. Changing the GHSV has two major effects in the CPO system. As the GHSV increases the axial velocity of the gas also increases. As the velocity increases, the contact time in the catalyst decreases. This leads to a lower conversion of methane, because all of the reactants do not diffuse to the surface quickly enough. However, the increased velocity leads to faster heat convection from the front to the back of the catalyst or from the combustion section to the reforming section. This leads to higher back face temperatures which favors the reforming reactions. Since the combustion reactions are so fast, it is the GHSV in the reforming section limiting the conversion. For the Pt/Ni catalyst, it may make more sense to have a longer reforming section and a shorter combustion section. This will alleviate the problem with a short GHSV in the reforming section. This problem does not arise for rhodium, because rhodium is an excellent combustion and reforming catalyst under these feed conditions.

4.2. Pt/Ni versus Ni/Pt

The Ni/Pt catalyst was investigated to assure the efficacy of placing a combustion catalyst before the reforming catalyst. This was shown by switching the order and placing the nickel reforming catalyst before the platinum combustion catalyst. In all cases, the Pt/Ni catalyst showed higher methane conversions, higher selectivities to hydrogen, and lower back face temperatures than the Ni/Pt catalyst. In addition, extended runs using the Ni/Pt catalyst were not carried out. It is anticipated that the nickel would have deactivated over time leaving a 5 mm platinum catalyst to carry out CPO. Initially, the catalyst would have been decent, but then the performance would have decreased substantially as the nickel deactivated.

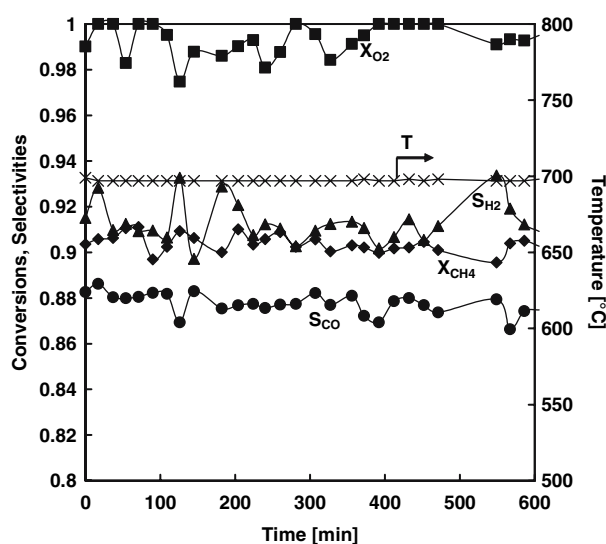


Figure 5. Feed conversions (oxygen ■ and methane ◆), product selectivities (hydrogen ▲ and carbon monoxide ●), and catalyst back face temperatures (x-secondary axis) as a function of time on-stream for a 10 h experiment.

4.3. Pt/Ni degradation

The experiment carried out for an extended time period showed absolutely no decrease in performance of the Pt/Ni catalyst. There was slight discoloration in the nickel catalyst over time. This could be due to phase changes, but nonetheless it did not affect the performance of the catalyst. The platinum catalyst showed no obvious signs of degradation.

5. Conclusions

We have demonstrated that a dual bed bimetallic catalyst composed of a combustion catalyst followed by a reforming catalyst demonstrates comparable methane conversion and hydrogen selectivity compared to best available catalysts in the literature over a wide range of GHSV's and feed compositions. The dual bed catalyst achieved hydrogen yields over 85% at a GHSV of 220,000 h⁻¹ using air as the oxidant. The dual bed catalyst cost approximately 40% of the cost of the rhodium catalyst.

In this work, the combustion catalyst and reforming catalyst each experienced the same GHSV. Investigation of the effects of changing the relative GHSV's for the two sections is currently in progress. Further investigations in this research will also investigate non-noble metal based combustion catalysts to greatly reduce the cost of the catalyst.

Acknowledgments

G.C.M.T would like to thank the Natural Sciences and Engineering Research Council (NSERC) of Canada for financial support through the Undergraduate Student Research Awards. J.F. would like to thank the Eugenie Ulmer Lamothe Scholarship Fund for financial support. C.A.L. would like to thank Dr. Karthik Venkataraman for valuable discussions regarding the manuscript.

References

- [1] M.V. Twigg, *Catalyst Handbook* (Wolfe, Frome, England, 1989).
- [2] A. Ashcroft, A. Cheetham, J. Foord, M. Green, C. Grey, A. Murrell and P. Vernon, *Nature* 344 (1990) 319.
- [3] V.R. Choudhary, A.M. Rajput and V.H. Rane, *J. Phys. Chem.* 96 (1992) 8686.
- [4] H.Y. Wang and E. Ruckenstein, *Catal. Lett.* 59 (1999) 121.
- [5] D.A. Hickman and L.D. Schmidt, *Science* 259 (1993) 343.
- [6] D.A. Hickman, E.A. Hauptfear and L.D. Schmidt, *Catal. Lett.* 17 (1993) 223.
- [7] C.A. Leclerc, R.M. Redenius and L.D. Schmidt, *Catal. Lett.* 79 (2002) 39.
- [8] K.A. Williams, C.A. Leclerc and L.D. Schmidt, *AIChE J.* 51 (2005) 247.
- [9] D.A. Hickman and L.D. Schmidt, *AIChE J.* 39 (1993) 1164.
- [10] G.A. Deluga, J.R. Salge, L.D. Schmidt and X.E. Verykios, *Science* 303 (2004) 993.
- [11] R.P. O'Connor, E.J. Klein and L.D. Schmidt, *Catal. Lett.* 70 (2000) 99.
- [12] L.D. Schmidt, E.J. Klein, C.A. Leclerc, J.J. Krummenacher and K.N. West, *Chem. Eng. Sci.* 58 (2003) 1037.
- [13] J.J. Krummenacher, K.N. West and L.D. Schmidt, *J. Catal.* 215 (2003) 332.
- [14] P.M. Torniaainen, X. Chu and L.D. Schmidt, *J. Catal.* 146 (1994) 1.
- [15] O.V. Buyevskaya, D. Wolf and M. Baerns, *Catal. Lett.* 29 (1994) 249.
- [16] E.P.J. Mallens, J.H.B.J. Hoebink and G.B. Marin, *J. Catal.* 167 (1997) 43.
- [17] J.H. Lee and D.L. Trimm, *Fuel Proc. Tech.* 42 (1995) 339.
- [18] D.A. Hickman and L.D. Schmidt, *J. Catal.* 138 (1992) 167.
- [19] U.S. Geological Survey, *Mineral Commodities Summaries 2004*, U.S. Department of the Interior (2004).
- [20] U.S. Geological Survey, *Metal Prices in the United States through 1998*, U.S. Department of the Interior (2004).
- [21] L. Ma and D.L. Trimm, *Appl. Catal. A: Gen.* 138 (1996) 265.
- [22] A.K. Avci, D.L. Trimm, A.E. Aksoylu and Z.I. Onsan, *Appl. Catal. A: Gen.* 258 (2004) 235.
- [23] J. Zhu, M.S.M. Mujeebur Rahuman, J.G. Van Ommen and L. Lefferts, *Appl. Catal. A: Gen.* 259 (2004) 95.